# NLoS Localization and UWB Channel Capacity Analysis

Von der Fakultät für Elektrotechnik und Informatik

der Gottfried Wilhelm Leibniz Universität Hannover
zur Erlangung des Grades eines

DOKTORS DER INGENIEURWISSENSCHAFTEN

Dr.-Ing.

genehmigte Dissertation
von

M.Sc Bamrung Tau Sieskul

geboren am 16.08.1979 in Lopburi in Thailand

2010

| | |
|---|---|
| Referent | **Prof. Dr.-Ing. Thomas Kaiser** |
| Referent | **Prof. Dr. H. Vincent Poor, Princeton University, USA** |
| Vorsitzender | **Prof. Dr.-Ing. Markus Fidler** |
| Tag der Promotion | **20. Mai 2010** |

Hannoversche Beiträge zur Nachrichtentechnik

Band 2.19

**Bamrung Tau Sieskul**

# NLoS Localization and UWB Channel Capacity Analysis

Shaker Verlag
Aachen 2010

**Bibliografische Information der Deutschen Nationalbibliothek**
Die Deutsche Nationalbibliothek verzeichnet diese Publikation in der Deutschen Nationalbibliografie; detaillierte bibliografische Daten sind im Internet über http://dnb.d-nb.de abrufbar.

Zugl.: Hannover, Leibniz Univ., Diss., 2010



ISBN 978-3-8322-9268-3
ISSN 1616-5489

Shaker Verlag GmbH • Postfach 101818 • 52018 Aachen
Telefon: 02407 / 95 96 - 0 • Telefax: 02407 / 95 96 - 9
Internet: www.shaker.de • E-Mail: info@shaker.de

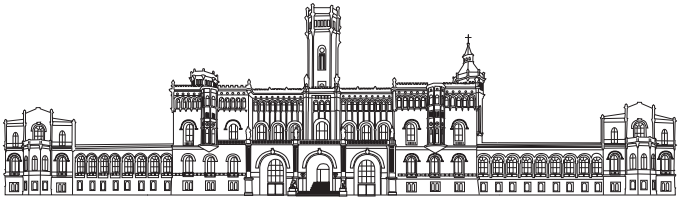

Institut für Kommunikations-Technik

Leibniz Universität Hannover

## KURZFASSUNG

Die vorliegende Dissertation hat die Lokalisierung und Kommunikation mittels Funk zum zentralen Inhalt: zum einen wird, basierend auf der Ankunftszeit (Time of Arrival, ToA) eines gesendeten Funksignals, die Position einer Mobilstation geschätzt und die Genauigkeit der Schätzung beurteilt. Zum anderen wird die Kanalkapazität von ultrabreitbandigen Mehrantennen-Nachrichtenkanälen berechnet um qualitative Aussagen über die erzielbare Datenrate zu gewinnen.

Im ersten Teil der Arbeit wird eine klassische ToA-Schätzmethode zusammen mit einem Pfadverlustmodel betrachtet. Es wird gezeigt, dass die Berücksichtigung der Pfadverluste die Genauigkeit der ToA-Schätzung erhöht unter der Voraussetzung, dass der Pfadverlustexponent (Path Loss Exponent, PLE) am Empfänger perfekt bekannt ist. Ausgehend von der sich ergebenden Leistungsverbesserung der ToA-Schätzung wird als konsequenter nachfolgender Schritt die *nicht perfekte* Kenntnis des PLEs am Empfänger untersucht. Hier zeigt sich, dass der Maximum-Likelihood-Schätzer (ML-Schätzer) von einer geringen deterministischen PLE-Störung bei einem kleinen Signal-zu-Rausch-Verhältnis (Signal-to-Noise-Ratio, SNR) profitiert. Weiterhin ergibt sich für die ML-Schätzung im Falle des nicht perfekten PLE ein kleinerer mittlerer quadratischer Fehler im Vergleich zum konventionellen Maximum-Correlation-Schätzer (MC-Schätzer), der keinerlei PLE-Kenntnis annimmt. Eine weitere Verallgemeinerung der ToA-Schätzung ergibt sich durch die Berücksichtigung eines komplexwertigen Pfadgewinns; es wird gezeigt, dass ein komplexwertiges Datenmodell ein entsprechendes reellwertiges Datenmodell um den Faktor $\frac{1}{4}$ im asymptotischen Fehlersinne übertrifft. Des Weiteren werden neue Algorithmen für die vorliegende Problemstellung vorgeschlagen und durch Berechnung der Cramer-Rao-Schranke eingehend analysiert.

Im zweiten Teil der Arbeit wird die Kapazität der Ultrabreitband-Kommunikation (UWB-Kommunikation) für einen standardisierten Kanal mit Cluster-Effekt abgeleitet und auf Mehrantennensysteme erweitert, wobei die Laufzeitverzögerungen der Antennenelemente mit berücksichtigt werden. Für unkorreliertes Fading sind die oberen Schranken sowie die Approximation der Kanalkapazität unabhängig von den Laufzeitverzögerungen der Antennenelemente. Die Kanalkapazität wächst zunächst mit der Anzahl der Pfade, um dann in eine Sättigung zu gehen. Die Kanalkapazität ist dann nahezu konstant und von der Anzahl der Pfade unabhängig. Darüber hinaus ist die Kanalkapazität der standardisierten NLoS-Kanalmodelle (Non-Line-of-Sight, NLoS) generell höher als die der standardisierten LoS-Kanalmodelle (Line-of-Sight, LoS).



**Schlagworte**: Parameterschätzung, Pfadverlust, Ultrabreitband.

ABSTRACT

This thesis deals with the localization and communication by means of radio signals. Based on the time-of-arrival (ToA), the first part of this thesis addresses the estimation of the position of a mobile station and the enhancement of the estimation accuracy. The second part of this thesis evaluates the channel capacity of the multiantenna ultrawideband communication channels in order to predict the achievable data rate.

In the first part, a classical ToA estimation approach is considered in conjunction with a path loss model. It is shown that the path loss exploitation increases the ToA estimation accuracy, provided that the path loss exponent (PLE) is perfectly known at the receiver. Apart from such prospect performance improvement, the performance of the geolocalization by exploiting the path attenuation information is also investigated when the PLE is not exactly known. It is found that for a small deterministic PLE error and a low signal-to-noise ratio, the maximum likelihood (ML) estimator can still benefit from the path loss model even when the the path loss model is subject to the uncertain PLE. More precisely, the ML estimator under the imperfect PLE can provide lower root mean square error than the conventional maximum correlation estimator, which does not require any PLE knowledge. The above results, which are obtained for real-valued data models, is then extended to complex-valued data models. It is found that a special complex data model outperforms the real data model by a factor $\frac{1}{4}$ in terms of the asymptotic error variance. Applying the ToA estimation with the path gain attenuation information to the wireless non-line-of-sight (NLoS) geolocation problem, we analyze the Cramér-Rao bound of the mobile position estimation.

In the second part, the channel capacity is derived for a standard channel including cluster feature, which is further extended to the multiantenna systems taking into account the propagation delay across antenna elements. For uncorrelated fading, the upper bounds and the approximate channel capacity using the determinant approximation do not depend on the antenna element time delay. The channel capacity increases with the number of rays. However, it will be saturated when the number of rays becomes sufficiently large. In addition, the channel capacity of the standard NLoS channel models is higher than that of the standard line-of-sight channel models.

**Keywords**: Parameter estimation, path loss, ultrawideband.

# ACKNOWLEDGEMENTS

The deepest appreciation is devoted to Prof. Dr.-Ing. Thomas Kaiser for giving a student an opportunity to pursue a doctoral degree in both Duisburg and Hannover. The research under Thomas' supervision is pleasant. My gratitude definitely is expressed to him for his kindness, patience, forgiveness, encouragement, inspiration, and etc. He helped the student even non-scientifically.

The author is grateful to Prof. Vincent Poor from Princeton University in New Jersey for accepting our invitation, his imperative suggestion to a flagship [1], and his time allocation to become a committee in the thesis defense. All of these are deeply appreciated by a student, since the Dean of School of Engineering and Applied Science would have a lot of duties to carry out.

Ganz herzlich bedanke ich mich bei Herrn Prof. Dr.-Ing. Markus Fidler für seine Zusage als der Vorsitzender der mündlichen Prüfung der Promotion.

During a long journey, even though difficult to thank fellow colleagues for what they contributed to someone, it is delightful to remember those who are involved with this thesis.

While was being with the Department of Communication Systems (Fachgebiet Nachrichtentechnische Systeme, NTS) at the University of Duisburg-Essen in Duisburg, a new-coming Ph.D. candidate has been indebted to all former and current NTS staffs, especially to Amr Eltaher for picking a new colleague up from the airport for the first time of arrival and later for introducing the works, events, and environment around Duisburg Campus, Qipeng Cai for some discussions regarding both technical and non-technical issues in the evening, Christane Senger for her cooperation and suggestions, Mr. Busch for accompanying a German-unspeakable foreigner to prolong the visa, Werner Stoppok, Wolfgang Krüll, and Barbara Brox for their explanation of the use of apparatus and shared computers, and Petra Kaiser for her manipulation of many documents and explanation of greeting words in Germany. As far as I can remember, the idea of the time-of-arrival estimation with the path loss model for the wireless NLoS geolocation has been suggested by Thomas, while we were moving from the NTS to the office of a new company in TecTrum at Bismarckstraße in Duisburg.

Hier in einer wunderschönen Stadt möchte ich mich ganz herzlich bei allen Mitarbeiterinnen und Mitarbeitern am Institut für Kommunikationstechnik an der Leibniz Universität Hannover für ihre Zusammenarbeit und ihre Unterstützungen bedanken. Dieser Dank gilt besonders Herrn Dittrich für die Schlüssel von Anfang an, Herrn Dipl.-Ing. Rolf Becker für das zusätzliche RAM im Rechner, Frau Schröder für ihre Verarbeitung der Vertragsverlängerungen, und Frau Adler für ihre Verarbeitung der Reiseanträge und der Reisekostenabrechnungen der Konferenzen.

Bei Frau Dipl.-Wirtsch.-Ing. Kim Bartke, Herrn M.Sc. Emil Dimitrov, Herrn Dr.-Ing. Mohamed El-Hadidy, und Herrn Dipl.-Wirtsch.-Ing. Henrik Schumacher bedanke ich mich herzlich während des Heckler&Koch-Projekts für die Zusammenarbeit. Für die Sprachverbesserung zum Thema Aspekte der Nachrichtenübertragungssysteme zur Studie „UWP—UWB auf der Picatinny Rail" bin ich Herrn Christoph Henning sehr dankbar. Am Projekt „EUWB - Coexisting Short Range Radio by Advanced Ultra-Wideband Radio Technology" bedanke ich mich ganz herzlich bei Frau Dipl.-Ing. Sondos Alaa, Frau Dipl.-Ing. Golaleh Rahmatollahi, Herrn M.Sc. Emil Dimitrov, und Herrn Dr.-Ing. Claus Kupferschmidt, der das Arbeitspacket 3 leitet, für die Meetings und Telefonkonferenz. Thanks also pass to Antti Antonnen and other project partners in the work packet 3.

Regarding the publications related to this thesis, the author is grateful to Associate Editiors and Reviewers for their efforts in evaluating and reviewing the submitted drafts, which have been notified as either acceptance or rejection, and Journal Coordinators for their proof versions before the actual publication. To sup-

port the community, thanks go to several Committees and Associate Editiors for their invitations to review until now 44 conference and 27 journal manuscripts.

One of the author's deep gratitude is expressed to Dr. Feng Zheng for his mathematical verification, other derivation techniques, wording improvement, conceptual comments, and responds to the reviewers' comments for several drafts. Without Dr. Feng, someone may still understand that the multiplication of two Gaussian random variables remains a Gaussian random variable. This thesis would never come to the end of the road without the encouragement from both Prof. Dr.-Ing. Thomas Kaiser and Dr. Feng Zheng and without the financial management by Dr.-Ing. Andreas Wilzeck.

Für die auf Deutsch verbesserte Kurzfassung in der Studienarbeit meiner Studentin bin ich Frau Dipl.-Ing. Sondos Alaa El Din, Herrn Dipl.-Wirtsch.-Ing. Christoph König, und Herrn M.Sc. Ralf Lübben sehr dankbar. Für die Vorlage dieser Dissertation bedanke ich mich herzlich bei Herrn Dipl.-Ing. Michael Bredel. A great gratitude is expressed to Peter for his suggestion to use the Laprint in creating several LaTeX built-in figures, which appear in most of the author's works. Special thanks are devoted to some nice colleagues at IKT, e.g., M.Eng. Wan Ibrahim Nurdiana, M.Sc. Anggia Anggraini, M.Sc. Hanwen Cao, M.Sc. Kiattisak Maichalernnukul, Dr. Hieu Nguyen, M.Sc. Trung Kien Nguyen, M.Sc. Zhao Zhao, and etc., for many interesting discussions.

Special appreciation is devoted to two students, M.Sc. Muhammad Saleem and T.E. María Isabel Valera Martínez, for conducting their theses with the author in Duisburg and Hannover, respectively. Thanks to both for spending some time in preparing the papers.

In the past five years, a life may be a bit lonely possibly due to the cold weather. Without the friendship from friends, the warmth to do the research would never exist. Thanks pass to all friends, e.g., Mr. Sakkasam Ratanathammapan, Mr. Piriya Taptimthong, Mr. Chumpon Pamornvisit, Miss Krittika Gosoomsawan, and etc., for some nice meals not only in both Duisburg and Hannover but also at other places and for sharing their experience around the world. In der Mandelslohstraße 2, 30419 Hannover bedanke ich mich bei einem netten Nachbar, der Jean-Christophe Schultze heißt, für unsere gemeinsame Zeit, Diskussionen, und seine Hilfe. Zum Kicken am jeden Mittwoch Abend bedanke ich mich herzlich bei Jens für seine Organisation und bei Henrik, Sebastian, Steve, und Timo für die Rückfahrt. Ebenso möchte ich mich bei Sanam, Amina, Chung, Sondos, Feng, und Claus für die gemeinsamen und witzigen Mittagessen in der Mensa bedanken.

Bei Claus, Henrik, und Herrn Kaiser möchte ich mich ganz herzlich für die auf Deutsch Kurzfassung dieser Dissertation bedanken. For the english version of the abstract of this thesis, deep appreciation is devoted to Dr. Feng.

Zur Veröffentlichung bei Shaker-Verlag-GmbH bedanke ich mich ganz herzlich bei Herrn Jansen für seine Probedrucke dieser Dissertation.

A large number of people and their contributions to this thesis may still be missing herein. Nevertheless, they are acknowledged in the author's mind.

Last but not least, the author is much obliged to the family, such as the father - Mr. Porn who has been forever unable to live with his family since last February, the mother - Mrs. Buasie, and the siblings, for allowing one of their members to be absent from home and for their patience due to different longitudes.

Bamrung Tau Sieskul
Hannover, im Juli 2010

To my family,
colleagues,
readers,
and those who may find it useful.

# PUBLICATIONS

## MAIN WORKS

Apart from the following publications, the contents of this thesis are drawn from some unpublished analyses and derivations.

*Conferences*

1. B. Tau Sieskul, F. Zheng, and T. Kaiser, "A hybrid SS-ToA wireless NLoS geolocation based on path attenuation: Mobile position estimation," *IEEE Wireless Communications & Networking Conference (WCNC)*, Budapest, Hungary, April 5-8, 2009, pp. 1-6.
2. B. Tau Sieskul, T. Kaiser, and F. Zheng, "A hybrid SS-ToA wireless NLoS geolocation based on path attenuation: Cramér-Rao bound," *IEEE 69th Vehicular Technology Conference (VTC2009-Spring)*, Barcelona, Spain, April 26-29, 2009, pp. 1-5.
3. B. Tau Sieskul, F. Zheng, and T. Kaiser, "Time-of-arrival estimation in path attenuation", *IEEE International Workshop on Signal Processing Advances for Wireless Communications (SPAWC)*, Perugia, Italy, June 21-24, 2009, pp. 573-577.
4. B. Tau Sieskul, C. Kupferschmidt, and T. Kaiser, "Algebraic inequalities for MIMO-UWB with antenna element time delays: Uncorrelated fading", *2009 IEEE International Conference on Ultra-Wideband (ICUWB 2009)*, Vancouver, Canada, September 9-11, 2009, pp. 798-803.

*Journals*

1. B. Tau Sieskul, F. Zheng and T. Kaiser, "On the effect of shadow fading on wireless geolocation in mixed LoS/NLoS environments," *IEEE Transactions on Signal Processing*, vol. 57, no. 11, pp. 4196-4208, Nov. 2009.
2. B. Tau Sieskul, F. Zheng and T. Kaiser, "A hybrid SS-ToA wireless NLoS geolocation based on path attenuation: ToA estimation and CRB for mobile position estimation," *IEEE Transactions on Vehicular Technology*, vol. 58, no. 9, pp. 4930-4942, Nov. 2009.

## RELATED WORKS

Under the roles of participant, editor, supervisor, and author, several works, which vary from slight to high relation to the topics in this thesis, have been conducted as follows.

*Technical Reports*

1. T. Kaiser, M. El-Hadidy, E. Dimitrov, und B. Tau Sieskul, „Ultrawideband auf der Picatinny-Rail—Kapitel 3: Aspekte der Nachrichtenübertragungssysteme," Heckler&Koch-Projekt, Studie zum Thema Interoperabilität System Soldat (SF163), Leibniz Universität Hannover, Hannover, Jul. 2007.
2. M. Chiani, M. Fabbri, A. Giorgetti, C. Kupferschmidt, S. A. El Din, and B. Tausieskul, "Application-specific channel modeling with spatial and tempo-

ral correlation analysis of the theoretical limits of MIMO-UWB," Integrated Project - EUWB, Tech. Rep. Deliverable D3.1.3, Jan. 2009.

*Supervised Theses*

1. M. Saleem, "Channel capacity assessment for the UWB wireless communication system in the presence of lognormal fading", in partial fulfillment of the requirements for the degree of Master of Science (M.Sc.) in Computer Science and Communication Engineering, Fachgebiet Nachrichtentechnische Systeme (Department of Communication Systems), Universität Duisburg-Essen (University of Duisburg-Essen), Duisburg, Mar. 2006.

2. M. I. Valera Martínez "A hybrid SS-ToA wireless geolcation based on path attenuation: Robustness investigation under imperfect path loss exponent," supported in part by the European Region Action Scheme for the Mobility of University Students (ERASMUS) for performing the Master's thesis at the Leibniz University of Hannover, Germany, in partial fulfilment of the requirements for the degree of Telecommunications Engineer at the Technical University of Cartagena, Spain, Aug. 2009.

*Conferences*

1. B. Tau Sieskul and T. Kaiser, "Cramér-Rao bound for TOA estimations in UWB positioning systems," *IEEE International Conference on Ultra-Wideband (ICU)*, Zurich, Switzerland, Sep. 2005, pp. 408-413.

2. T. Kaiser and B. Tau Sieskul, "An Introduction to multiple antennas for UWB communication and localization," *Conference on Information Sciences and Systems (CISS)*, Princeton, NJ, March 2006, pp. 638-643.

3. M. Saleem, B. Tau Sieskul, and T. Kaiser, "Channel capacity assessments in UWB communication system over lognormal fading," *IEE Symposium on Ultra Wideband Systems, Technologies and Applications*, London, UK, April, 2006, pp. 155-159.

4. T. Kaiser, C. Senger, and B. Tau Sieskul, "Antenna arrays for UWB indoor localization in non-line of sight environments," invited paper, *IEEE MTT-S International Microwave Symposium*, San Francisco, CA, June, 2006.

5. M. I. Valera Martínez, B. Tau Sieskul, F. Zheng, and T. Kaiser, "A hybrid SS-ToA wireless geolocation based on path attenuation under imperfect path loss exponent," *18th European Signal Processing Conference 2010 (EUSIPCO-2010)*, August 2010, accepted for presentation.

6. B. Tau Sieskul, C. Kupferschmidt, and T. Kaiser, "Spatial fading correlation for semicircular scattering: Angular spread and spatial frequency approximations," *3rd International Conference on Communications and Electronics 2010 (ICCE 2010)*, August 2010, accepted for presentation.

*Journals*

1. T. Kaiser, C. Senger, J. Schroeder, S. Galler, E. Dimitrov, M. El-Hadidy and B. Tau Sieskul, "Ultra-wideband wireless systems: A broad review," *The Radio Science Bulletin*, no. 320, pp. 25-39, March, 2007.

2. B. Tau Sieskul, C. Kupferschmidt, and T. Kaiser, "Spatial fading correlation for local scattering: A condition of angular distribution," *IEEE Transactions on Vehicular Technology*, Feb. 2010, second revision.

*Book Chapters*

1. T. Kaiser, C. Senger, A. Eltaher, and B. Tau Sieskul, Localization in non-line-of-sight scenarios with ultra-wideband antenna arrays, in *Ultra Wideband: Antennas and Propagation for Communications, Radar and Imaging*, edited by B. Allen, M. Dohler, E. E. Okon, W. Q. Malik, A. K. Brown, and D. J. Edwards, John Wiley & Sons, 2007.

2. T. Kaiser, F. Zheng, B. Tau Sieskul, and K. Maichalernnukul, An Overview of UWB Systems with MIMO, in *Short-Range Wireless Communications Emerging Technologies and Applications*. Edited by R. Kraemer and M. D. Katz, ch. 9, pp. 65-72, John Wiley & Sons, 2009.

3. B. Tau Sieskul, F. Zheng, and T. Kaiser, Mobile Position Estimation Using Time of Arrival in Mixed LOS/NLOS Environments, in *Position Location - Theory, Practice and Advances: A Handbook for Engineers and Academics*. Edited by S. Zekavat and M. Buehrer, under review, 2010.

Listings xxix
1 Introduction 1
1.1 Literature Reviews . . . 1
1.1.1 Backgrounds . . . 1
1.1.2 Wireless NLoS Geolocation . . . 2
1.1.3 UWB Channel Capacity . . . 10
1.1.4 Gap . . . 17
1.1.5 Relation . . . 18
1.2 Objectives . . . 18
1.3 Scope . . . 18
1.4 Problem Statement . . . 18
1.4.1 Problem . . . 18
1.4.2 Significance . . . 18
1.5 Novelties, Contributions, and Merits . . . 18
1.5.1 Novelties . . . 19
1.5.2 Contributions . . . 19
1.5.3 Merits . . . 19
1.6 Organization . . . 19

I TIME-OF-ARRIVAL ESTIMATION IN PATH ATTENUATION 21
2 Maximum Likelihood Estimator 23
2.1 Introduction . . . 23
2.1.1 Literature Reviews . . . 23
2.1.2 Motivation . . . 23
2.1.3 Scope . . . 23
2.1.4 Contributions . . . 24
2.1.5 Organization . . . 24
2.2 Transceiver Model . . . 24
2.2.1 Transmitted Signal Assumptions . . . 24
2.2.2 Path Loss Model . . . 26
2.2.3 Received Signal Model . . . 26
2.2.4 Additive Noise Assumptions . . . 26
2.2.5 Channel Assumptions . . . 27
2.2.6 Discrete-time Representation . . . 27
2.3 Error Expansion . . . 28
2.4 Maximum Correlation . . . 28
2.4.1 MC Estimator . . . 28
2.4.2 Asymptotic Performance of the MC Estimator . . . 28
2.5 Maximum Likelihood . . . 29
2.5.1 ML Estimator . . . 29
2.5.2 Asymptotic Performance of the ML Estimator . . . 30
2.6 Cramér-Rao Bound for ToA Estimation . . . 30
2.7 Relative Performance . . . 30
2.8 Numerical Results . . . 30
2.8.1 OFDM Signal . . . 31
2.8.2 Link Budget . . . 31
2.8.3 MC Implementation . . . 32
2.8.4 Numerical Examples . . . 32
2.9 Concluding Remarks and Future Directions . . . 34

3 Imperfect Path Loss Exponent 37
3.1 Introduction . . . 37
3.2 Deterministic Imperfect PLE . . . 38
3.2.1 Performance Degradation . . . 40
3.2.2 Upper Bound for Small Absolute Value of PLE Error . . . 41
3.3 Stochastic Imperfect PLE . . . 41
3.3.1 Randomly Guessed PLE . . . 42
3.3.2 Randomly True PLE . . . 43
3.4 Bias Reduction . . . 43
3.4.1 PLE Estimation using the MC Estimator . . . 44
3.4.2 Bias Reduction using the BCML Estimator . . . 44
3.5 Numerical Examples . . . 44
3.6 Conclusions . . . 48
4 Complex Signal 53
4.1 Introduction . . . 53
4.1.1 Literature Reviews . . . 53
4.1.2 Gap . . . 54
4.1.3 Scope . . . 54
4.1.4 Merits and Contributions . . . 54
4.1.5 Basic Algebraic Results . . . 54
4.1.6 Organization . . . 55
4.2 Complex-valued Transceiver Model . . . 55
4.3 Complex-valued Path Gain in Cartesian Form . . . 56
4.4 Complex-valued Path Gain in Polar Form . . . 58
4.4.1 Noise Variance Estimation and Concentrated Likelihood . . . 59
4.4.2 Unstructured Model: ML Estimator and CRB . . . 60
4.4.3 Path Loss Model with Perfect PLE: ML Estimator and CRB . . . 61
4.4.4 Path Loss Model with Unknown PLE: ML Estimator and CRB 61
4.4.5 Path Loss Model with Imperfect PLE: Error Analysis . . . 62
4.4.6 Approximate CRB . . . 71
4.5 Numerical Examples . . . 72
4.5.1 OFDM Signal Energy . . . 72
4.5.2 Maximum Complex Correlation Estimator . . . 81
4.6 Conclusions . . . 82

II HYBRID SS-TOA WIRELESS NLOS GEOLOCATION 83
5 Cramér-Rao Bound for Mobile Position Estimation 85
5.1 Introduction . . . 85
5.1.1 Literature Reviews . . . 85
5.1.2 Motivation . . . 86
5.1.3 Scope and Gap . . . 86
5.1.4 Merit and Contributions . . . 86
5.1.5 Organization . . . 86
5.2 System Model . . . 87
5.3 CRB for Mobile Position Estimation . . . 89
5.4 Numerical Examples . . . 91
5.5 Concluding Remarks and Future Directions . . . 93
6 Mobile Position Estimation 97
6.1 Introduction . . . 97
6.1.1 Literature Reviews . . . 97
6.1.2 Merits . . . 97
6.1.3 Organization . . . 98
6.2 Mobile Position Estimation . . . 98
6.2.1 Least Squares . . . 99
6.2.2 Weighted Least Squares . . . 99
6.2.3 Maximum Likelihood . . . 99
6.2.4 Error Variance of the Position Estimate Using Least Squares . 100

6.3 CRB for the Mobile Position Estimation . . . 100
6.3.1 CRB for the ToA Estimation . . . 100
6.3.2 CRB for the Mobile Position Estimation . . . 101
6.4 Numerical Examples . . . 101
6.5 Concluding Remarks . . . 103
7 Shadowing Effects 105
7.1 Introduction . . . 105
7.1.1 Research Gap . . . 106
7.1.2 Contribution . . . 106
7.1.3 Organization . . . 106
7.2 System Model . . . 107
7.3 Deterministic Shadowing . . . 109
7.3.1 CRB for the Mobile Position Estimation . . . 110
7.3.2 Inherent Accuracy Behavior . . . 111
7.4 Random Shadowing . . . 113
7.4.1 Asymptotic CRB . . . 114
7.4.2 Modified CRB with Nuisance Elimination . . . 114
7.4.3 Simplified Bayesian CRB . . . 115
7.4.4 Bayesian CRB . . . 117
7.5 Numerical Examples . . . 119
7.6 Concluding Remarks and Future Works . . . 121

III CHANNEL MODELING AND CHANNEL CAPACITY IN UWB COMMUNICATIONS 125
8 Multiantenna Ultrawideband Channel: Modeling and Capacity Analysis 127
8.1 Introduction . . . 127
8.1.1 Motivation . . . 127
8.1.2 Novelty, Merits, and Contributions . . . 128
8.1.3 Notations . . . 128
8.1.4 Organization . . . 128
8.2 Frequency-Selective MIMO Channel Capacity . . . 128
8.2.1 Ergodic Capacity . . . 129
8.2.2 Power Constraint . . . 129
8.2.3 Power Spectral Density Constraint . . . 129
8.3 IEEE 802.15.4a Channel Model . . . 129
8.4 Multiantenna Channel Model . . . 131
8.4.1 Antenna Element Propagation Delay . . . 131
8.4.2 Effective Channel Model . . . 132
8.4.3 Random Parameters . . . 132
8.5 Uncorrelated Noise and Signal . . . 133
8.6 Inequalities . . . 134
8.6.1 Jensen Upper Bound . . . 134
8.6.2 Determinant Upper Bounds . . . 134
8.6.3 Trace Upper Bounds . . . 135
8.7 Channel Statistics . . . 135
8.7.1 Amplitude Correlation . . . 135
8.7.2 PDP Expectation . . . 136
8.8 Upper Bounds . . . 138
8.9 Numerical Examples . . . 138
8.10 Concluding Remarks and Future Directions . . . 139

IV CONCLUSIONS AND FUTURE WORKS 141
9 Conclusions and Future Works 143

A Algebraic Derivations 145
A.1 Proof of Lemma 2 . . . 145
A.2 Proof of Proposition 1 . . . 146
A.3 Proof of Proposition 2 . . . 146
A.4 Proof of Theorem 1 . . . 147
A.5 Proof of Lemma 3 . . . 147
A.6 Proof of Proposition 3 . . . 148
A.7 Proof of Lemma 4 . . . 149
A.8 Proof of Lemma 5 . . . 150
A.9 Proof of Lemma 6 . . . 152
A.10 Proof of Lemma 7 . . . 153
A.11 Proof of Proposition 4 . . . 154
A.12 Proof of Proposition 5 . . . 155
A.13 Proof of Proposition 6 . . . 155
A.14 Proof of Proposition 7 . . . 157
A.15 Proof of Proposition 8 . . . 158
A.16 Proof of Lemma 8 . . . 158
A.16.1 The First-order Derivatives . . . 160
A.16.2 The Second-order Derivatives . . . 161
A.17 Proof of Corollary 1 . . . 170
A.18 Proof of Corollary 2 . . . 170
A.19 Proof of Lemma 9 . . . 171
A.20 Proof of Lemma 10 . . . 172
A.21 Proof of Lemma 11 . . . 172
A.21.1 Maximum Likelihood Estimator . . . 172
A.21.2 Cramér-Rao Bound . . . 174
A.22 Proof of Lemma 12 . . . 175
A.22.1 Maximum Likelihood Estimator . . . 175
A.22.2 Cramér-Rao Bound . . . 176
A.23 Proof of Lemma 13 . . . 176
A.23.1 Maximum Likelihood Estimator . . . 176
A.23.2 Cramér-Rao Bound . . . 177
A.24 Error Analysis of the ML Estimator under Imperfect PLE . . . 179
A.24.1 Expectation of the Absolute Value of the Correlation between the Received Signal and the Transmitted Signal at the True ToA 181
A.24.2 Expectation of the Square of the Absolute Value of the Correlation between the Received Signal and the Transmitted Signal at the True ToA . . . 183
A.24.3 Expectation of A Product of the Absolute Value of the Correlation between the Received Signal and the Transmitted Signal and Its Derivative at the True ToA . . . 184
A.24.4 Expectation of the Square of the Derivative of the Absolute Value of the Correlation between the Received Signal and the Transmitted Signal at the True ToA . . . 186
A.24.5 Expectation of the First Derivative of the Absolute Value of the Correlation between the Received Signal and the Transmitted Signal at the True ToA . . . 205
A.24.6 Expectation of the Second Derivative of the Absolute Value of the Correlation between the Received Signal and the Transmitted Signal at the True ToA . . . 209
A.25 Proof of Lemma 14 . . . 214
A.26 Proof of Lemma 15 . . . 214
A.27 Proof of Lemma 16 . . . 225
A.28 Proof of Lemma 17 . . . 229
A.28.1 Calculation of $\check{E}_{ss}(\tau)$ . . . 229
A.28.2 Calculation of $\check{E}_{s\dot{s}}(\tau)$ . . . 231
A.28.3 Calculation of $\check{E}_{\dot{s}\dot{s}}(\tau)$ . . . 232

A.28.4 Calculation of $\check{E}_{s\tilde{s}}(\tau)$ . . . 233
A.29 Proof of Proposition 12 . . . 234
A.29.1 Derivation of Two Jacobian Matrices . . . 234
A.29.2 CRB Derivation . . . 235
A.30 Proof of Remark 6 . . . 244
A.31 Proof of Remark 7 . . . 244
A.32 Proof of Lemma 18 . . . 244
A.33 Proof of Proposition 13 . . . 246
A.34 Proof of Proposition 14 . . . 246
A.35 Proof of Lemma 19 . . . 247
A.36 Proof of Lemma 20 . . . 247
A.37 Proof of Proposition 16 . . . 248
A.38 Proof of Lemma 21 . . . 253
A.39 Proof of Proposition 17 . . . 255
A.40 Proof of Lemma 22 . . . 256

BIBLIOGRAPHY 259

Figure 1 Effective bandwidth of the transmitted singal as a function in the symbol duration for several numbers of the OFDM sub-carriers with $N_R = 10$ independent runs . . . . . 32

Figure 2 RMSE of the position estimate as a function of the signal-to-noise ratio $\frac{E_{ss}}{\sigma_n^2}$ (dB) for $\gamma = 4.5425$, $d = 1{,}000$ m, $T_s = 10^{-3}$ sec, $\bar{\beta} = 3.6517 \times 10^4$ Hz, sampling time $= 3.7037 \times 10^{-9}$ sec, and $N_R = 1{,}000$ independent runs. . . . . 33

Figure 3 RMSE of the position estimate as a function of the signal duration $T_s$ (sec) for $\gamma = 4.5425$, $d = 1{,}000$ m, $10\log_{10}\left(\frac{E_{ss}}{\sigma_n^2}\right) = 150$ dB, sampling time $= \frac{1}{2.5\times10^5}T_o$ sec, and $N_R = 1{,}000$ independent runs. . . . . 34

Figure 4 RMSE of the position estimate as a function of the PLE $\gamma$ for $\bar{\beta} = 3.6517 \times 10^4$ Hz, $d = 1{,}000$ m and $10\log_{10}\left(\frac{E_{ss}}{\sigma_n^2}\right) = 150$ dB, $T_s = 10^{-3}$ sec, sampling time $= \frac{1}{2\times10^6}T_o$ sec, and $N_R = 100$ independent runs. . . . . 35

Figure 5 RMSE of the position estimate as a function of the distance d (m) for $\bar{\beta} = 3.6517 \times 10^4$ Hz, $\gamma = 4.5425$, $10\log_{10}\left(\frac{E_{ss}}{\sigma_n^2}\right) = 150$ dB, $T_s = 10^{-3}$ sec, sampling time $= \frac{1}{2\times10^6}T_o$ sec, and $N_R = 100$ independent runs. . . . . 35

Figure 6 Bias as a function of the received SNR $\frac{E_{ss}}{\sigma_n^2}a^2(\tau_0|\gamma_0)$ with $f_0 = 1.9$ GHz, $d_0 = 100$ m, $d = 1{,}000$ m, $\gamma_0 = 2$, $\delta_\gamma = 0.1\gamma_0$, $N = 2^5$ OFDM sub-carriers, $T_s = 10^{-3}$ sec, sampling time $= \frac{1}{10^3}\tau_0$, $T_o = \tau_0 + T_s$, and $N_R = 1{,}000$ independent runs. . . 45

Figure 7 RMSE as a function of the received SNR $\frac{E_{ss}}{\sigma_n^2}a^2(\tau_0|\gamma_0)$ with $f_0 = 1.9$ GHz, $d_0 = 100$ m, $d = 1{,}000$ m, $\gamma_0 = 2$, $\delta_\gamma = 0.1\gamma_0$, $N = 2^5$ OFDM sub-carriers, $T_s = 10^{-3}$ sec, sampling time $= \frac{1}{10^3}\tau_0$, $T_o = \tau_0 + T_s$, and $N_R = 1{,}000$ independent runs. . . 46

Figure 8 Bias as a function of the PLE error $\delta_\gamma$ with $f_0 = 1.9$ GHz, $d_0 = 100$ m, $d = 1{,}000$ m, $N = 2^6$ OFDM sub-carriers, $T_s = 10^{-3}$ sec, sampling time $= \frac{1}{10^3}\tau_0$, $T_o = \tau_0 + T_s$, received SNR $\frac{E_{ss}}{\sigma_n^2}a^2(\tau_0|\gamma_0) = 19$ dB, $\gamma_0 = 2$, and $N_R = 1{,}000$ independent runs. . . . . 47

Figure 9 RMSE as a function of the PLE error $\delta_\gamma$ with $f_0 = 1.9$ GHz, $d_0 = 100$ m, $d = 1{,}000$ m, $N = 2^6$ OFDM sub-carriers, $T_s = 10^{-3}$ sec, sampling time $= \frac{1}{10^3}\tau_0$, $T_o = \tau_0 + T_s$, received SNR $\frac{E_{ss}}{\sigma_n^2}a^2(\tau_0|\gamma_0) = 19$ dB, $\gamma_0 = 2$, and $N_R = 1{,}000$ independent runs. . . . . 48

Figure 10 Bias as a function of the PLE $\gamma_0$ with $f_0 = 1.9$ GHz, $d_0 = 100$ m, $d = 1{,}000$ m, $N = 2^6$ OFDM sub-carriers, $T_s = 10^{-3}$ sec, sampling time $= \frac{1}{10^3}\tau_0$, $T_o = \tau_0 + T_s$, received SNR $\frac{E_{ss}}{\sigma_n^2}a^2(\tau_0|\gamma_0) = 19$ dB, $\delta_\gamma = 0.05\gamma_0$, and $N_R = 1{,}000$ independent runs. . . . . 49

Figure 11 RMSE as a function of the PLE $\gamma_0$ with $f_0 = 1.9$ GHz, $d_0 = 100$ m, $d = 1{,}000$ m, $N = 2^6$ OFDM sub-carriers, $T_s = 10^{-3}$ sec, sampling time $= \frac{1}{10^3}\tau_0$, $T_o = \tau_0 + T_s$, received SNR $\frac{E_{ss}}{\sigma_n^2}a^2(\tau_0|\gamma_0) = 19$ dB, $\delta_\gamma = 0.05\gamma_0$, and $N_R = 1{,}000$ independent runs. . . . . 50

Figure 12 Probability of improvement $\Pr\left\{\mathrm{E}_{n(t)}\left\{(\hat{\tau}_{\mathrm{ML}}(\gamma)-\tau_0)^2\right\} \leqslant \mathrm{E}_{n(t)}\left\{(\hat{\tau}_{\mathrm{MC}}-\tau_0)^2\right\}\right\}$ as a function of the standard deviation of the untruncated Gaussian PLE, $\sigma_\gamma$, with $f_0 = 1.9$ GHz, $d_0 = 100$ m, $d = 1{,}000$ m, $N = 2^5$ OFDM sub-carriers, $T_s = 10^{-3}$ sec, sampling time $= \frac{1}{10^3}\tau_0$, $T_o = \tau_0 + T_s$, transmitted SNR $\frac{E_{ss}}{\sigma_n^2} = 146$ dB, $\gamma_{\min} = 3.7$ & $\gamma_{\max} = 6.5$ (urban macrocell [2, p. 47]), $\bar{\gamma} = 4.6 - 0.0075\left(\frac{1}{2}(80+10)\right) + \frac{1}{\frac{1}{2}(80+10)}12.6 = 4.5425$ (a hilly/moderate-to-heavy tree density [3]), $\gamma \sim \mathcal{N}_{\gamma_{\min}}^{\gamma_{\max}}(\bar{\gamma}, \sigma_\gamma^2)$, $\gamma_0 = \bar{\gamma}$, $N_R = 50$ independent runs, and $N_\gamma = 50$ independent samples. . . . . 50

Figure 13 Probability of improvement $\Pr\left\{\mathrm{E}_{n(t)}\left\{(\hat{\tau}_{\mathrm{ML}}(\gamma)-\tau_0)^2\right\} \leqslant \mathrm{E}_{n(t)}\left\{(\hat{\tau}_{\mathrm{MC}}-\tau_0)^2\right\}\right\}$ as a function of the standard deviation of the untruncated Gaussian PLE, $\sigma_\gamma$, with $f_0 = 1.9$ GHz, $d_0 = 100$ m, $d = 1{,}000$ m, $N = 2^5$ OFDM sub-carriers, $T_s = 10^{-3}$ sec, sampling time $= \frac{1}{10^3}\tau_0$, $T_o = \tau_0 + T_s$, transmitted SNR $\frac{E_{ss}}{\sigma_n^2} = 150$ dB, $\gamma_{\min} = 3.7$ & $\gamma_{\max} = 6.5$ (urban macrocell [2, p. 47]), $\bar{\gamma} = 4.6 - 0.0075\left(\frac{1}{2}(80+10)\right) + \frac{1}{\frac{1}{2}(80+10)}12.6 = 4.5425$ (a hilly/moderate-to-heavy tree density [3]), $\gamma \sim \mathcal{N}_{\gamma_{\min}}^{\gamma_{\max}}(\bar{\gamma}, \sigma_\gamma^2)$, $\gamma_0 = \frac{1}{2}(\gamma_{\max} + \gamma_{\min})$, $N_R = 50$ independent runs, and $N_\gamma = 50$ independent samples. . . . . 51

Figure 14 Probability of improvement $\Pr\left\{\mathrm{E}_{n(t)}\left\{(\hat{\tau}_{\mathrm{ML}}(\gamma)-\tau_0)^2\right\} \leqslant \mathrm{E}_{n(t)}\left\{(\hat{\tau}_{\mathrm{MC}}-\tau_0)^2\right\}\right\}$ as a function of the standard deviation of the untruncated Gaussian PLE, $\sigma_\gamma$, with $f_0 = 1.9$ GHz, $d_0 = 100$ m, $d = 1{,}000$ m, $N = 2^5$ OFDM sub-carriers, $T_s = 10^{-3}$ sec, sampling time $= \frac{1}{10^3}\tau_0$, $T_o = \tau_0 + T_s$, transmitted SNR $\frac{E_{ss}}{\sigma_n^2} = 145$ dB, $\gamma_{\min} = 3.7$ & $\gamma_{\max} = 6.5$ (urban macrocell [2, p. 47]), $\bar{\gamma} = 4.6 - 0.0075\left(\frac{1}{2}(80+10)\right) + \frac{1}{\frac{1}{2}(80+10)}12.6 = 4.5425$ (a hilly/moderate-to-heavy tree density [3]), $\gamma_0 \sim \mathcal{N}_{\gamma_{\min}}^{\gamma_{\max}}(\bar{\gamma}, \sigma_\gamma^2)$, $\gamma = \bar{\gamma}$, $N_R = 50$ independent runs, and $N_{\gamma_0} = 50$ independent samples. . . . . 51

Figure 15 Probability of improvement $\Pr\left\{\mathrm{E}_{n(t)}\left\{(\hat{\tau}_{\mathrm{ML}}(\gamma)-\tau_0)^2\right\} \leqslant \mathrm{E}_{n(t)}\left\{(\hat{\tau}_{\mathrm{MC}}-\tau_0)^2\right\}\right\}$ as a function of the standard deviation of the untruncated Gaussian PLE, $\sigma_\gamma$, with $f_0 = 1.9$ GHz, $d_0 = 100$ m, $d = 1{,}000$ m, $N = 2^5$ OFDM sub-carriers, $T_s = 10^{-3}$ sec, sampling time $= \frac{1}{10^3}\tau_0$, $T_o = \tau_0 + T_s$, transmitted SNR $\frac{E_{ss}}{\sigma_n^2} = 146$ dB, $\gamma_{\min} = 3.7$ & $\gamma_{\max} = 6.5$ (urban macrocell [2, p. 47]), $\bar{\gamma} = 4.6 - 0.0075\left(\frac{1}{2}(80+10)\right) + \frac{1}{\frac{1}{2}(80+10)}12.6 = 4.5425$ (a hilly/moderate-to-heavy tree density [3]), $\gamma_0 \sim \mathcal{N}_{\gamma_{\min}}^{\gamma_{\max}}(\bar{\gamma}, \sigma_\gamma^2)$, $\gamma = \frac{1}{2}(\gamma_{\min} + \gamma_{\max})$, $N_R = 50$ independent runs, and $N_{\gamma_0} = 50$ independent samples. . . . . 52

Figure 16 The energy $E_{ss}(\tau_0)$ of the OFDM signal as a function of the ratio between the observation period and the symbol duration $\frac{T_o}{T_s}$ with $N = 2^5$ OFDM sub-carriers, $d = 1{,}000$ m, $T_s = 10^{-3}$ sec, sampling time $= \frac{1}{2\times 10^3}\tau_0$ sec, and $N_R = 100$ independent runs. . . . . 78

Figure 17 The correlation $\Re\left(E_{ss}(\tau_0)\right)$ of the OFDM signal as a function of the ratio between the observation period and the symbol duration $\frac{T_o}{T_s}$ with $N = 2^5$ OFDM sub-carriers, $d = 1{,}000$ m, $T_s = 10^{-3}$ sec, sampling time $= \frac{1}{2\times 10^3}\tau_0$ sec, and $N_R = 100$ independent runs. . . . . 79

Figure 18 The correlation $\Im\left(E_{s\ddot{s}}(\tau_0)\right)$ of the OFDM signal as a function of the ratio between the observation period and the symbol duration $\frac{T_o}{T_s}$ with $N = 2^5$ OFDM sub-carriers, $d = 1{,}000$ m, $T_s = 10^{-3}$ sec, sampling time $= \frac{1}{2\times10^3}\tau_0$ sec, and $N_R = 100$ independent runs. . . . . 79
Figure 19 The energy $E_{s\ddot{s}}(\tau_0)$ of the OFDM signal as a function of the ratio between the observation period and the symbol duration $\frac{T_o}{T_s}$ with $N = 2^5$ OFDM sub-carriers, $d = 1{,}000$ m, $T_s = 10^{-3}$ sec, sampling time $= \frac{1}{2\times10^3}\tau_0$ sec, and $N_R = 100$ independent runs. . . . . 80
Figure 20 The energy $E_{s\ddot{s}}(\tau_0)$ of the OFDM signal as a function of the ratio between the observation period and the symbol duration $\frac{T_o}{T_s}$ with $N = 2^5$ OFDM sub-carriers, $d = 1{,}000$ m, $T_s = 10^{-3}$ sec, sampling time $= \frac{1}{2\times10^3}\tau_0$ sec, and $N_R = 1$ independent runs. . . . . 80
Figure 21 The energy $E_{ss}(\tau)$ of the OFDM signal as a function of the ToA $\tau$ for the ratio between the observation period and the symbol duration of 1.2, i.e., $\frac{T_o}{T_s} = 1.2$, with $N = 2^5$ OFDM sub-carriers, $d = 1{,}000$ m, $T_s = 10^{-3}$ sec, sampling time $= \frac{1}{2\times10^3}\tau_0$ sec, and $N_R = 173$ independent runs. . . . . 81
Figure 22 Cellular system with cell radius r. . . . . 92
Figure 23 Cramér-Rao lower bound as a function of the effective bandwidth for several PLEs with $SNR_{dB} = 110$ dB, number of BSs $B = 7$, number of BSs receiving NLoS signals $M = 3$, close-in distance $d_0 = 4$ m, and cell radius $r = 20$ m. . . . . 93
Figure 24 Cramér-Rao lower bound as a function of the PLE for several cell radii with $SNR_{dB} = 120$ dB, effective bandwidth $\bar{\beta} = \frac{1}{\sqrt{3}}5$ MHz, number of BSs $B = 7$, number of BSs receiving NLoS signals $M = 3$, and close-in distance $d_0 = 4$ m. . . . . 94
Figure 25 Cramér-Rao lower bound as a function of the signal-to-noise ratio for several cell radii with effective bandwidth $\bar{\beta} = \frac{1}{\sqrt{3}}5$ GHz, number of BSs $B = 7$, number of BSs receiving NLoS signals $M = 3$, PLE $\gamma = 2.55$, and close-in distance $d_0 = 4$ m. 95
Figure 26 Cramér-Rao lower bound as a function of cell radius for several numbers of the NLoS BSs with signal-to-noise ratio $SNR_{dB} = 100$ dB, number of BSs $B = 7$, $\gamma = 2.55$, and close-in distance $d_0 = 4$ m. . . . . 95
Figure 27 Cramér-Rao lower bound as a function of the number of the NLoS BSs for several close-in distances with effective bandwidth $\bar{\beta} = \frac{1}{\sqrt{3}}5$ MHz, number of BSs $B = 7$, signal-to-noise ratio $SNR_{dB} = 80$ dB, and cell radius $r = 20$ m. . . . . 96
Figure 28 RMSE of the position estimate as a function of the transmitted SNR for $M = 0$ NLoS BSs, $\bar{\beta} = \frac{1}{\sqrt{3}}10\pi$ MHz, $r = 2{,}000$ m, $\gamma_b = 4.5425$, and $N_R = 10{,}000$ independent runs. . . . . 102
Figure 29 RMSE of the position estimate as a function of the effective bandwidth of the transmitted signal for $\frac{E_s}{\sigma_n^2} = 90, 120, 150$ dB, $M = 1$ NLoS BSs, $r = 2{,}000$ m, $\gamma_b = 4.5425$, and $N_R = 100$ independent runs. . . . . 103
Figure 30 RMSE of the position estimate as a function of the number of the NLoS BSs for $\frac{E_s}{\sigma_n^2} = 120$ dB, $\bar{\beta} = \frac{1}{\sqrt{3}}10\pi$ MHz, $r = 2{,}000$ m, $\gamma_b = 4.5425$, and $N_R = 10{,}000$ independent runs. . . . . 104
Figure 31 RMSE of the position estimate as a function of the cell radius for $\frac{E_s}{\sigma_n^2} = 120$ dB, $\bar{\beta} = \frac{1}{\sqrt{3}}10\pi$ MHz, $M = 2$ NLoS BSs, $\gamma_b = 4.5425$, and $N_R = 10{,}000$ independent runs. . . . . 104

Figure 32 The CRB in (7.24) and $\tilde{\rho}$ in (7.29) as functions of the additional NLoS path length $l$. The terrain A and $M = 1$ are considered. Left plots invoke $\bar{\beta} = 18.138$ kHz. Right plots adopt $\bar{\beta} = 18.138$ MHz. . . . . 119
Figure 33 The CRB in (7.24) as a function of the number of the BSs B. . . 121
Figure 34 The CRB in (7.24) as a function of the shadow fading $\xi$. . . . 122
Figure 35 The ACRB in (7.46) and the SBCRB in (7.56) as a function of $\sigma_\sigma$. The corresponding parameters are set up as follows: $\bar{\beta} = \frac{1}{\sqrt{3}} 10\pi$ MHz, SNR $= 100$ dB, $B = 6$, $M = 1$, $r = 2{,}000$ m, $l = 10$ m, $f_0 = 1.9$ GHz, and $d_0 = 100$ m. . . . . 123
Figure 36 The positioning accuracy as a function of SNR. The corresponding parameters are set up as follows: $\bar{\beta} = \frac{1}{\sqrt{3}} 10\pi$ MHz, $B = 6$, $M = 1$, $r = 2{,}000$ m, $l = 10$ m, $f_0 = 1.9$ GHz, and $d_0 = 100$ m. . . . . 123
Figure 37 Channel capacity as a function of the number of summations M with $K = 100$, $\frac{\sigma_s^2}{\sigma_n^2} = 1$ (SNR = 0 dB), and all relevant parameters according to the CM1 (residential) for LoS scenario [4, Tbl. I]. . . . . 139
Figure 38 Channel capacity as a function of the number of the rays K with $M = 50$, $\frac{\sigma_s^2}{\sigma_n^2} = 1$ (SNR = 0 dB), and all relevant parameters according to the CM1 (residential) for LoS scenario [4, Tbl. I]. . . . . 140
Figure 39 Channel capacity as a function of the SNR $\frac{\sigma_s^2}{\sigma_n^2}$ with $M = 50$, $K = 100$, $N_r = N_t = 2$, and all relevant parameters according to the CM5 and CM6 for the LoS and the NLoS scenarios [4, Tbl. III]. . . . . 140

# LIST OF TABLES

Table 1 Comparison of deterministic bounds [5]. . . . . 4
Table 2 Analogy between deterministic bounds and Weiss-Weinstein family bounds [5]. . . . . 4

| | |
|---|---|
| AoA | angle of arrival |
| AoD | angle of departure |
| ACRB | asymptotic Cramér-Rao bound |
| AETD | antenna element time delay |
| BCML | bias-corrected maximum likelihood |
| BCRB | Bayesian Cramér-Rao bound |
| BS | base station |
| CDMA | Code Division Multiple Access |
| CM | channel model |
| CRB | Cramér-Rao bound |
| CSI | channel state information |
| DoA | direction of arrival |
| DS | direct sequence |
| EML | even maximum likelihood |
| FFT | fast Fourier transform |
| FIM | Fisher information matrix |
| IML | imperfect maximum likelihood |
| KL | Karhunen-Loève |
| LAN | local area network |
| LoS | line of sight |
| LLS | linearized least squares |
| LS | least squares |
| MC | maximum correlation |
| MCRB | modified Cramér-Rao bound |
| MFIM | modified Fisher information matrix |
| MIMO | multiple-input multiple-output |
| ML | maximum likelihood |
| MS | mobile station |
| MSE | mean square error |
| NLoS | non-line of sight |
| OFDM | orthogonal frequency division multiplexing |
| OML | odd maximum likelihood |
| PAM | pulse amplitude modulation |

| | |
|---|---|
| pdf | probability density function |
| PDP | power delay profile |
| PLE | path loss exponent |
| PPM | pulse position modulation |
| PSD | power spectral density |
| PSK | phase shift keying |
| QAM | quadrature amplitude modulation |
| QPSK | quadrature phase shift keying |
| RMS | root mean square |
| RMSE | root mean square error |
| SBCRB | simplified Bayesian Cramér-Rao bound |
| SNR | signal-to-noise ratio |
| SS | signal strength |
| TH | time hopping |
| ToA | time of arrival |
| TDoA | time difference of arrival |
| UWB | ultra-wideband |
| WLS | weighted least squares |

Some notations are described together with their first appearances as follows.

| | |
|---|---|
| $\mathbf{1}_{B-M}$ | column vector whose entries are $B-M$ ones in (7.29) |
| $a$ | amplitude or path gain in (1.1) |
| $a[k,l]$ | tap weight of the k-th component in the l-th cluster in (8.7) |
| $a_b$ | path gain to the b-th BS in (5.5) |
| $\hat{a}_{MC}$ | MC estimate of the path gain in (3.35) |
| $\mathbf{a}$ | vector of path gains from all multipath components in (1.12) |
| $\mathbf{a}$ | vector of path gains from all BSs in (6.15) |
| $\mathbf{a}$ | vector defined in (8.25a) |
| $\bar{\mathbf{a}}$ | vector of LoS path gains in (6.18a) |
| $\hat{\mathbf{a}}_{ML}$ | ML estimator of the path gains from all multipath components in (1.17) |
| $\mathbf{A}$ | matrix defined in (8.26a) |
| $\mathbf{A}[k,l]$ | matrix defined in (8.27a) |
| $\mathbf{A}(\tilde{p})$ | matrix defined in (7.25) |
| $\bar{\mathbf{A}}$ | matrix defined in (7.34) |
| $\tilde{\mathbf{A}}[k,l]$ | dispersion matrix of the amplitude matrix in Sec. 8.7.1 |
| $b$ | index of the b-th BS in (5.1) |
| $b_k$ | complex data symbol at the k-th sub-carrier in (2.39) |
| $b_{\tau\tau}$ | CRB of the ToA estimation in (4.12) |
| $b_{\tau\tau\|\hat{\alpha}}$ | CRB for unstructured complex-valued model in polar form in (4.26b) |
| $b_{\tau\tau\|\gamma}$ | CRB for complex-valued path loss model with perfect PLE in (4.30) |
| $b_{\tau\tau\|\hat{\gamma}}$ | CRB for complex-valued path loss model with unknown PLE in (4.32b) |
| $B$ | number of BSs in (5.1) |
| $\bar{B}_{det}$ | determinant uper bound on channel capacity in (8.37) |
| $\bar{B}_{Jensen}$ | Jensen upper bound on channel capacity in (8.36) |
| $\bar{B}_{tr}$ | upper bound based on trace inequality in (8.41) |
| $\bar{B}_{tr+Jensen}$ | upper bound based on trace and Jensen's inequalities in (8.41) |
| $\mathbf{B}[k,l]$ | matrix defined in (8.33) |
| $\mathbf{B}_{\boldsymbol{\tau\tau}}$ | matrix of CRB on ToA error variances in (6.16) |
| $\mathbf{B}_{\mathbf{pp}}$ | matrix of CRB on position error variances in (6.17) |
| $\tilde{\mathbf{B}}_{\mathbf{pp}}$ | error covariance matrix by modified CRB in (7.52) |
| $\check{\mathbf{B}}_{\mathbf{pp}}$ | error covariance matrix by simplified Bayesian CRB in (7.56) |
| $\check{\mathbf{B}}_{\mathbf{pp}}$ | error covariance matrix by Bayesian CRB in (7.65) |
| $\overline{\mathbf{B}}_{\mathbf{pp}}$ | error covariance matrix by asymptotic CRB in (7.46) |
| $c$ | speed of the light in (2.8) |
| $c_1$ | constant defined in (4.61) |
| $c_2$ | constant defined in (4.61) |
| $c_3$ | constant defined in (4.61) |
| $c_4$ | constant in (8.39) |
| $C$ | channel capacity in (1.30) |
| $\bar{C}$ | ergodic capacity in Sec. 8.2.1 |
| $\tilde{C}$ | approximate channel capacity in (8.40) |
| $\tilde{C}_{approdet}$ | approximate channel capacity after inserting the expectation in (8.40) |
| $\mathbf{C}$ | set of complex number |
| $d$ | distance between the transmitter and the receiver in (2.8) |
| $d$ | distance of adjacent antenna element separation in Sec. 8.4.1 |
| $d_0$ | close-in reference distance in (2.8) |

$d_b[i]$ the i-th range measurement to the b-th station in (1.18)
$\mathbf{d}_b$ vector of the position of the b-th station in (1.22c)
$\check{\mathbf{d}}$ vector taken from the distances between $B - M$ LoS BSs and the MS
$\check{\mathbf{d}}$ vector of distances between M NLoS BSs and the MS in (7.30a)
$\mathbf{D}(\cdot)$ diagonal matrix whose diagonal elements are given by the vector $\cdot$
$\mathbf{e}_b$ error vector in (1.22e)
$E$ received energy
$E_b$ received energy at the b-th BS in (5.2)
$E_h$ channel energy related to (1.35)
$E_s$ transmitted energy from the mobile station in (5.2)
$E_{ss}$ the energy of the signal in (2.2)
$E_{ss}(\tau)$ exact signal energy as a function of the ToA in (4.6)
$E_{s\dot{s}}(\tau)$ correlation between the transmitted signal and its derivative in (4.7)
$E_{\dot{s}\dot{s}}(\tau)$ correlation between the derivatives of the transmitted signal in (4.8)
$E_{\dot{s}_R\dot{s}_R}(\tau_0)$ correlation between the derivatives of the real parts of signal in (4.13a)
$E_{\dot{s}_I\dot{s}_I}(\tau_0)$ correlation between the derivatives of the imaginary parts of signal in (4.13b)
$E_{s_Rs_R}(\tau_0)$ correlation between the real parts of signal in (4.13c)
$E_{s_Is_I}(\tau_0)$ correlation between the imaginary parts of signal in (4.13d)
$E_{s_R\dot{s}_R}(\tau_0)$ correlation between real part and its derivative in (4.13e)
$E_{s_I\dot{s}_R}(\tau_0)$ correlation between imaginary part and the derivative of real part in (4.13f)
$E_{s_R\dot{s}_I}(\tau_0)$ correlation between real part and the derivative of imaginary part in (4.13g)
$E_{s_I\dot{s}_I}(\tau_0)$ correlation between imaginary part and its derivative in (4.13h)
$\check{E}_{ss}(\tau)$ signal energy defined in (4.47a)
$\check{E}_{s\dot{s}}(\tau)$ signal energy defined in (4.47b)
$\check{E}_{\dot{s}\dot{s}}(\tau)$ signal energy defined in (4.47c)
$\check{E}_{s\ddot{s}}(\tau)$ signal energy defined in (4.47d)
$E_{ss}(\tau, \acute{\tau})$ signal energy defined in (1.16b)
$\mathbf{E}_{ss}(\boldsymbol{\tau}, \boldsymbol{\tau})$ matrix of signal correlations in (1.15b)
$f_0$ central frequency in (2.8)
$f_{b,k}(t)$ orthonormal function at the b-th BS in (5.10)
$f_k$ central frequency in (2.39)
$f_k(t)$ orthonormal function in (2.14)
$f_H$ highest frequency of signal which is at least 10 dB below the peak in Sec. 1.1.1
$f_L$ lowest frequency of signal which is at least 10 dB below the peak in Sec. 1.1.1
$f_{ML}(\boldsymbol{\eta})$ ML objective as a function of $\boldsymbol{\eta}$ in (4.23)
$f_{ML}(\tau|\gamma)$ ML function written as a function of $\tau$ conditioned on $\gamma$ in (3.1)
$g(\xi, \omega)$ quantity defined in (7.64b)
$g_{\xi}(\xi)$ quantity defined in (7.64a)
$h(t)$ channel impulse response in (8.7)
$h(\xi, \omega)$ quantity defined in (7.63b)
$h_{\sigma_n^2\sigma_n^2}$ Fisher information of noise variance in (4.20)

| | |
|---|---|
| $h_{\tau\tau\|\hat{\alpha}}$ | Fisher information in (4.27) |
| $h_{\xi}(\xi)$ | quantity defined in (7.63a) |
| $h^{k,l}_{n_r,n_t}(t)$ | channel of AETD in (8.20) |
| $h_{n_r,n_t}(t)$ | effective channel impulse response in (8.22) |
| $\overline{h}_{\xi,\xi}$ | modified Fisher information of $\xi$ in (7.55) |
| $\widetilde{h}_{\xi,\xi}$ | quantity defined in (7.62) |
| $\overline{\tilde{\mathbf{h}}}_{\boldsymbol{\tau}\xi}$ | modified Fisher information vector for NLoS in Sec. 7.4.3 |
| $\overline{\tilde{\mathbf{h}}}_{\boldsymbol{\tau}\xi}$ | modified Fisher information vector for LoS in Sec. 7.4.3 |
| $\mathbf{H}(t)$ | MIMO channel matrix in (8.1) |
| $\mathbf{H}_{K,L}(f)$ | channel matrix in frequency domain with $K+1$ clusters and $L+1$ rays in (8.32) |
| $\mathbf{H}_{[}(f)$ | Fourier transform of the channel matrix in (8.3) |
| $\mathbf{H}_{\mathbf{uu}}$ | Fisher information matrix in (7.47) |
| $\mathbf{H}_{\boldsymbol{\tau\tau}}$ | Fisher information matrix in (6.14) |
| $\mathbf{H}_{\boldsymbol{\theta\theta}}$ | Fisher information matrix in (4.17) |
| $\breve{\mathbf{H}}_{\boldsymbol{\theta\theta}}$ | total information matrix in (7.59) |
| $\overline{\mathbf{H}}_{\mathbf{uu}}$ | modified FIM in (7.49) |
| $\overline{\mathbf{H}}_{\boldsymbol{\theta\theta}}$ | modified FIM of model parameter in 7.54 |
| $\overline{\tilde{\mathbf{H}}}_{\boldsymbol{\tau\tau}}$ | modified FIM for NLoS ToAs in (7.51a) |
| $\overline{\tilde{\mathbf{H}}}_{\boldsymbol{\tau\tau}}$ | modified FIM for LoS ToAs in (7.51b) |
| $\widetilde{\mathbf{H}}_{\boldsymbol{\theta\theta}}$ | *a priori* information matrix in (7.59) |
| $I_0(x)$ | zeroth order modified Bessel functions of the first kind in (4.48a) |
| $I_k(x)$ | k-th order modified Bessel functions of the first kind in (4.48a) |
| $\mathbf{I}_{(\cdot)}$ | identity matrix of size $\cdot$ in (8.2) |
| $k_1$ | constant defined in (4.61) |
| $k_m$ | mean factor defined in (8.10a) |
| $k_\gamma$ | parameter describing the increase in the decay constant with the delay in (8.18) |
| $\tilde{k}_m$ | standard deviation factor defined in (8.10b) |
| $K$ | $K+1$ is the number of rays in (8.7) |
| $l(\tau\|r(t);\, t\in(0,T_o])$ | likelihood function in logarithm scale in (2.20) |
| $l_b$ | additional path length caused by the NLoS propagation in (5.3) |
| $\ell(\tau_b\|r_b(t);\, t\in(0,T_o])$ | likelihood function in logarithm scale in (5.16) |
| $l_{\acute{m},m}(\mathbf{y})$ | likelihood ratio in (1.37) |
| $\mathbf{l}$ | vector of additional path lengths caused by NLoS propagation in (5.7) |
| $L$ | $L+1$ is the number of clusters in (8.7) |
| $\bar{L}$ | mean of $L$ in (8.8) |
| $\tilde{L}$ | number of multipath components in Theorem 3 |
| $m$ | m-factor of Nakagami distribution in (8.9) |
| $M$ | number of BSs that are subject to the NLoS propagation |
| $M$ | large number for approximating the infinite sum in Sec. 8.9 |
| $M_c$ | shadowing exponent in (8.19) |
| $\mathbf{M}(f)$ | matrix defined in (8.3) |
| $n$ | index of sampling point in (7.14) |
| $n(t)$ | additive noise at the receiver at time $t$ in (1.1) |

| | |
|---|---|
| $n_b(t)$ | additive noise at the b-th BS in (5.5) |
| $n_{b,k}$ | noise sample at the b-th BS in (5.13) |
| $n_I(t)$ | imaginary part of the noise $n(t)$ in (4.10f) |
| $n_k$ | noise sample in (2.18b) |
| $n_p$ | index of multipath component in (1.7) |
| $n_r$ | index of antenna element at the receiver in Sec. 8.4.1 |
| $n_R(t)$ | real part of the noise $n(t)$ in (4.10e) |
| $n_t$ | index of antenna element at the transmitter in Sec. 8.4.1 |
| $\mathbf{n}(t)$ | additive noise at the receiver in (8.1) |
| $N$ | the number of measurements in (1.18) |
| $N$ | number of complex data symbols per block in (2.39) |
| $N_0$ | double-sided power spectral density |
| $N_o$ | number of observed samples after sampling in (7.14) |
| $N_p$ | number of multipath components in (1.7). |
| $N_r$ | number of antenna elements at the receiver in Sec. 8.2 |
| $N_s$ | number of samples at which the transmitted signal is nonzero in (7.16) |
| $N_t$ | number of antenna elements at the transmitter in Sec. 8.2 |
| $\tilde{N}$ | number of random parameters in Sec. 8.2.1 |
| $\check{N}$ | minimum number between the numbers of the transmitter and receiver antennas in (8.2) |
| $\mathcal{N}$ | set of BS indices that are subject to the NLoS propagation |
| $o(\cdot)$ | little 'o' of Bachmann-Landau symbols in (2.21) |
| $O(\cdot)$ | big 'o' of Bachmann-Landau symbols in (8.38) |
| $\Omega$ | mean square value of the amplitude in (8.9) |
| $p(r_1, \ldots, r_K\|\tau)$ | conditional pdf of the received signal samples in (2.19) |
| $p(r_{b,1}, \ldots, r_{b,K}\|\tau_b)$ | conditional pdf of received signal samples at the b-th BS in (5.15) |
| $p_{\mathbf{r}\|\mathbf{u}}(\mathbf{r}\|\mathbf{u})$ | marginal pdf in (7.48) |
| $p_{\mathbf{r}\|\mathbf{v},\mathbf{u}}(\mathbf{r}\|\mathbf{v},\mathbf{u})$ | conditional pdf in (7.48) |
| $p_{\mathbf{v}}(\mathbf{v})$ | pdf of $\mathbf{v}$ in (7.48) |
| $p(\mathbf{x},\mathbf{y})$ | joint pdf of $\mathbf{x}$ and $\mathbf{y}$ in (1.36) |
| $\mathbf{p}$ | position of the MS in (5.7) |
| $\mathbf{p}_b$ | the b-th BS position in (5.1) |
| $\hat{\mathbf{p}}_{LS}$ | position estimate using the LS criterion in (6.8) |
| $\hat{\mathbf{p}}_{ML}$ | position estimate using the ML criterion in (6.10) |
| $\hat{\mathbf{p}}_{WLS}$ | position estimate using the WLS criterion in (6.9) |
| $\check{\mathbf{p}}$ | a guessed value of the true position in Sec. 1.1.2 |
| $P$ | limited power for transmission in (8.5) |
| $\mathbf{P}$ | matrix of all BS positions in (5.30) |
| $\hat{\mathbf{q}}_{LLS}$ | vector defined in (1.27) |
| $Q(\cdot)$ | transition probability function related to (1.35) |
| $r$ | cell radius in (5.30) |
| $r(t)$ | received signal at time $t$ in (2.9) |
| $r_b(t)$ | received signal at the b-th BS in (5.5) |
| $r_{b,k}$ | received signal sample at the b-th BS in (5.12) |

| | |
|---|---|
| $r_I(t)$ | imaginary part of the received signal $r(t)$ in (4.10b) |
| $r_k$ | received signal sample in (2.16) |
| $r_R(t)$ | real part of the received signal $r(t)$ in (4.10a) |
| $\mathbf{r}(t)$ | vector of received signals from all BSs in (5.17) |
| $\mathbb{R}_+$ | set of positive number |
| $R(f)$ | Fourier transform of $r(t)$ in (2.43) |
| $\mathbf{R_{nn}}(\tau)$ | noise autocovariance matrix in (8.28) |
| $\mathbf{R_{xx}}(\tau)$ | transmitted signal autocovariance matrix in (8.30) |
| $s(t)$ | transmitted signal in (2.1) |
| $s_{b,k}$ | signal sample at the b-th BS in (5.13) |
| $s_I(t)$ | imaginary part of the transmitted signal $s(t)$ in (4.10d) |
| $s_k$ | signal sample in (2.18a) |
| $s_R(t)$ | real part of the transmitted signal $s(t)$ in (4.10c) |
| $\dot{s}(t)$ | derivative of the signal $s(t)$ with respect to the time $t$ in (1.6) |
| $\mathbf{s}(t, \boldsymbol{\tau})$ | vector of delayed transmitted signals in (7.8c) |
| $\tilde{\mathbf{s}}(t; \boldsymbol{\tau}, \xi)$ | composite signal defined in (7.20) |
| $\tilde{s}(t)$ | OFDM signal in (2.39) |
| $S(f)$ | Fourier transform of the transmitted signal $s(t)$ in (2.6) |
| SNR | SNR in (1.4) |
| $\text{SNR}_{\text{dB}}$ | SNR in decibel in (2.42) |
| $\widetilde{\text{SNR}}_b$ | received SNR at the b-th BS |
| $t$ | time on the real line |
| $T[l]$ | the l-th cluster arrival time in (8.7) |
| $T_s$ | signal duration in Sec. 1.1.2 |
| $T_o$ | observation period in (2.2) |
| $T_f$ | frame period (1.35) |
| $u$ | Gaussian random variable only in (7.40) |
| $\mathbf{u}$ | deterministic parameter in Sec. 7.4.2 |
| $v$ | Gaussian random variable only in (7.41) |
| $\mathbf{v}$ | random parameter in Sec. 7.4.2 |
| $w(t)$ | signal waveform in (2.1) |
| $W$ | bandwidth in Sec. 1.1.1 |
| $\bar{\mathbf{W}}$ | weighting matrix corresponding to LoS portion in (6.9) |
| $x$ | x coordinate of the MS in x-y plane in (5.8) |
| $x_0$ | true value of $x$ in (5.22) |
| $x_b$ | x coordinate of the b-th BS in x-y plane in (5.1) |
| $\tilde{x}_b$ | relative distance in the x-axis between the b-th BS and the MS in (5.3) |
| $\mathbf{x}(t)$ | transmitted signal at the transmitter in (8.1) |
| $y$ | y coordinate of the MS in x-y plane in (5.8) |
| $y_0$ | true value of $y$ in (5.22) |
| $y_b$ | y coordinate of the b-th BS in x-y plane in (5.1) |
| $\tilde{y}_b$ | relative distance in the y-axis between the b-th BS and the MS in (5.3) |
| $\mathbf{y}(t)$ | received signal at the receiver in (8.1) |
| $\alpha$ | amplitude of complex path gain in (4.18) |
| $\alpha_b$ | quantity defined in (5.28) |

| | |
|---|---|
| $\alpha_b$ | real path gain with shadow fading in (7.6) |
| $\alpha_{n_r,n_t}[k,l]$ | antenna-dependent complex amplitude in (8.23) |
| $\boldsymbol{\alpha}$ | vector of path gains from all BSs in (7.8b) |
| $\beta$ | effective bandwidth in (1.5) |
| $\beta$ | frequency band |
| $\beta$ | mixture probability parameter in (8.14) |
| $\bar{\beta}$ | Gabor's effective bandwidth in (2.6) |
| $\bar{\beta}_c$ | critical effective bandwidth in (7.31) |
| $\chi_b$ | quantity defined in (5.24a) |
| $\chi$ | attenuation factor of the first component in (8.15) |
| $\delta$ | Nyquist sampling period in (7.14) |
| $\delta(t)$ | Dirac delta function in (8.7) |
| $\delta_{\cdot,\cdot}$ | Kronecker delta function |
| $(\delta_x,\delta_y)$ | the corresponding guessed error pair in Sec. 1.1.2 |
| $\delta_\gamma$ | PLE error in (3.6) |
| $\check{\delta}_\gamma$ | upper limit of the confident PLE difference in (3.20) |
| $\boldsymbol{\delta}$ | vector defined in (8.25e) |
| $\hat{\boldsymbol{\delta}}_{LLS}$ | linearlized least squares estimate in (1.23) |
| $\boldsymbol{\Delta}$ | matrix defined in (1.22a) |
| $\epsilon$ | ratio of total positioning errors in (7.39) |
| $\epsilon(\tau\|\gamma)$ | bias in parametric form in (3.32) |
| $\overline{\epsilon}$ | statistical mean of $\epsilon$ in (7.43) |
| $\bar{\epsilon}$ | empirical error variance in (6.22) |
| $\epsilon^2$ | total positioning accuracy in (5.22) |
| $\eta_b$ | delay in discrete time in (7.16) |
| $\boldsymbol{\eta}$ | vector of random parameters in Sec. 8.2.1 |
| $\hat{\boldsymbol{\eta}}_{ML}$ | ML estimate of $\boldsymbol{\eta}$ in (4.22) |
| $\gamma$ | path loss exponent |
| $\gamma_0$ | true value of the PLE in (2.25) |
| $\gamma_1$ | parameter determining the decay at later times in (8.15) |
| $\gamma_b$ | PLE at the b-th BS in (5.2) |
| $\gamma_{max}$ | maximum value of the truncated random PLE in (3.23) |
| $\gamma_{min}$ | minimum value of the truncated random PLE in (3.23) |
| $\gamma_{MC}(\tau)$ | PLE estimate based on the MC estimator in (3.33) |
| $\gamma_r$ | parameter determining how fast the PDP increases to its local maximum in (8.15) |
| $\gamma_t$ | mean of the truncated Gaussian PLE in (3.24) |
| $\bar{\gamma}$ | mean of the untruncated random PLE in (3.23) |
| $\hat{\gamma}_{MC}$ | PLE estimate using the MC estimator in (3.36) |
| $\hat{\gamma}_{ML}$ | PLE estimate using the ML estimator in (3.3) |
| $\tilde{\gamma}_t$ | mean of the truncated Gaussian PLE in (3.28) |
| $\tilde{\gamma}_0$ | root for a condition of $\gamma_0$ in (3.31) |
| $\gamma[l]$ | intra-cluster decay time constant in (8.15) |
| $\boldsymbol{\gamma}$ | vector of the PLEs from all BSs in (6.6b) |
| $\bar{\boldsymbol{\gamma}}$ | vector of LoS PLEs in (6.18b) |
| $\Gamma(\cdot)$ | gamma function in (8.9) |

| | |
|---|---|
| $\iota$ | sign of the amplitude in (8.11) |
| $\kappa$ | constant depending on antenna characteristics and average channel attenuation in (2.8) |
| $\kappa_{dB}$ | constant $\kappa$ in decibel in (2.42) |
| $\lambda_1$ | a ray arrival rate in (8.14) |
| $\lambda_2$ | another ray arrival rate in (8.14) |
| $\lambda_{b,k}$ | eigenvalue of homogeneous Fredholm integral at the $b$-th BS in (5.10) |
| $\lambda_k$ | eigenvalue of homogeneous Fredholm integral in (2.14) |
| $\Lambda[l]$ | cluster arrival rate in (8.13) |
| $\mu_0$ | mean factor defined in (8.10a) |
| $\mu_m(\tau)$ | mean of lognormal random variable in (8.10a) |
| $\mu_\sigma$ | mean of $\sigma$ in (7.41) |
| $\tilde{\mu}_0$ | standard deviation factor defined in (8.10a) |
| $\nu$ | constant in (7.37) |
| $\Omega[l]$ | energy of the $l$-th cluster in (8.15) |
| $\phi$ | phase shift of complex path gain in (4.18) |
| $\phi$ | AoA in Sec. 8.4.1 |
| $\phi_b$ | relative angle between the $b$-th BS and the MS in (5.24b) |
| $\boldsymbol{\phi}$ | vector of relative angles in (5.32) |
| $\boldsymbol{\phi}$ | vector defined in (8.25c) |
| $\Phi(\cdot)$ | normal cumulative distribution function in (3.27) |
| $\boldsymbol{\Phi}$ | matrix defined in (8.26c) |
| $\boldsymbol{\Phi}[k,l]$ | matrix defined in (8.27c) |
| $\boldsymbol{\Phi}_{xx}$ | limited PSD matrix of a certain regulation in (8.6) |
| $\bar{\boldsymbol{\Phi}}$ | matrix taken from the last $B-M$ columns of $\boldsymbol{\Phi}$ in (6.4) |
| $\psi_{n_r,n_t}[k,l]$ | propagation delay across antenna element in (8.20) |
| $\boldsymbol{\Psi}(\tilde{\rho})$ | matrix defined in (7.28) |
| $\rho$ | average SNR related to (1.35) |
| $\sigma$ | standard deviation of $\tilde{\sigma}$ in (7.40) |
| $\sigma \sim \mathcal{N}(\mu_\sigma, \sigma_{\tilde{\sigma}}^2)$ | $\sigma$ is distributed as real Gaussian random variable with mean $\mu_\sigma$ and variance $\sigma_{\tilde{\sigma}}^2$ |
| $\sigma \sim \mathcal{N}_{\gamma_{min}}^{\gamma_{max}}(\mu_\sigma, \sigma_{\tilde{\sigma}}^2)$ | $\sigma$ is distributed as real truncated Gaussian random variable with untruncated mean $\mu_\sigma$ and untruncated variance $\sigma_{\tilde{\sigma}}^2$ within $[\gamma_{min}, \gamma_{max}]$ |
| $\boldsymbol{\Pi}_{xx}(f)$ | Fourier transform of the transmitted signal correlation matrix in (1.38) |
| $\boldsymbol{\Pi}_{nn}(f)$ | Fourier transform of the noise covariance matrix in (1.38) |
| $\rho_{ns}(\tau)$ | correlation between the noise and the transmitted signal in (2.35) |
| $\rho_{n\dot{s}}(\tau)$ | correlation between the noise and the derivative of the transmitted signal in (2.25) |
| $\rho_{rs}(\tau)$ | correlation between the received signal and the transmitted signal delayed with $\tau$ in (2.23) |
| $\tilde{\rho}$ | quantity defined in (7.29) |
| $\check{\rho}$ | quantity defined in (7.57) |
| $\check{\rho}$ | quantity defined in (7.66) |
| $\boldsymbol{\rho}_{rs}(\boldsymbol{\tau})$ | vector of the correlations in (1.15a) |
| $\tilde{\sigma}$ | shadowing exponent in (7.37) |

| | |
|---|---|
| $\sigma_c$ | standard deviation of shadowing exponent in (8.19) |
| $\sigma_\sigma$ | standard deviation of $\sigma$ in (7.41) |
| $\sigma_\infty$ | infinite summation of PDP in (8.45) |
| $\breve{\sigma}_{1,1}$ | an element of $\breve{\mathbf{\Sigma}}^{-1}$ in (4.58) |
| $\breve{\sigma}_{1,2}$ | an element of $\breve{\mathbf{\Sigma}}^{-1}$ in (4.58) |
| $\breve{\sigma}_{1,3}$ | an element of $\breve{\mathbf{\Sigma}}^{-1}$ in (4.58) |
| $\breve{\sigma}_{1,4}$ | an element of $\breve{\mathbf{\Sigma}}^{-1}$ in (4.58) |
| $\breve{\sigma}_{2,2}$ | an element of $\breve{\mathbf{\Sigma}}^{-1}$ in (4.58) |
| $\breve{\sigma}_{2,3}$ | an element of $\breve{\mathbf{\Sigma}}^{-1}$ in (4.58) |
| $\breve{\sigma}_{2,4}$ | an element of $\breve{\mathbf{\Sigma}}^{-1}$ in (4.58) |
| $\breve{\sigma}_{3,3}$ | an element of $\breve{\mathbf{\Sigma}}^{-1}$ in (4.58) |
| $\breve{\sigma}_{3,4}$ | an element of $\breve{\mathbf{\Sigma}}^{-1}$ in (4.58) |
| $\breve{\sigma}_{4,4}$ | an element of $\breve{\mathbf{\Sigma}}^{-1}$ in (4.58) |
| $\breve{\sigma}_{1\|3}(\tau_0)$ | a quantity defined in (4.59) |
| $\breve{\sigma}_{2\|3}(\tau_0)$ | a quantity defined in (4.59) |
| $\breve{\sigma}_{4\|3}(\tau_0)$ | a quantity defined in (4.59) |
| $\breve{\sigma}_{1,2\|3}(\tau_0)$ | a quantity defined in (4.59) |
| $\breve{\sigma}_{1,4\|3}(\tau_0)$ | a quantity defined in (4.59) |
| $\breve{\sigma}_{2,4\|3}(\tau_0)$ | a quantity defined in (4.59) |
| $\breve{\sigma}_{1\|4}(\tau_0)$ | a quantity defined in (4.59) |
| $\breve{\sigma}_{2\|4}(\tau_0)$ | a quantity defined in (4.59) |
| $\breve{\sigma}_{3\|4}(\tau_0)$ | a quantity defined in (4.59) |
| $\breve{\sigma}_{1,2\|4}(\tau_0)$ | a quantity defined in (4.59) |
| $\breve{\sigma}_{1,3\|4}(\tau_0)$ | a quantity defined in (4.59) |
| $\breve{\sigma}_{2,3\|4}(\tau_0)$ | a quantity defined in (4.59) |
| $\sigma_b^2$ | error variance of ToA from the $b$-th BS in (6.6c) |
| $\sigma_n^2$ | the variance of the noise sample in (2.19) |
| $\sigma_\gamma^2$ | variance of the random PLE in (3.22) |
| $\sigma_{\gamma_t}^2$ | variance of the truncated Gaussian PLE in (3.25) |
| $\tilde{\sigma}_{\gamma_t}^2$ | variance of the truncated Gaussian PLE in (3.29) |
| $\hat{\sigma}_n^2$ | estimate of noise variance in (4.20) |
| $\tilde{\boldsymbol{\sigma}}^2$ | vector the ToA error variances taken from all LoS BSs in (6.6c) |
| $\mathbf{\Sigma_{AA}}[k, l, \acute{k}, \acute{l}]$ | covariance matrix of the amplitude matirx in (8.42) |
| $\mathbf{\Sigma_{nn}}(f)$ | PSD matrix of the additive noise in (8.3) |
| $\mathbf{\Sigma_{xx}}(f)$ | PSD matrix of the transmitted signal in (8.2) |
| $\breve{\mathbf{\Sigma}}$ | matrix defined in (4.57) |
| $\tau$ | time delay in (1.1) |
| $\tau[k, l]$ | the delay of the $k$-th multipath component relative to the $l$-th cluster arrival time $T[l]$ in (8.7) |
| $\tau_0$ | true value of the ToA in (2.25) |
| $\tau_b$ | ToA at the $b$-th BS in (5.3) |
| $\hat{\tau}_{BCML}(\gamma)$ | parametric estimate of the ToA using the BCML estimator in (3.37) |
| $\hat{\tau}_{EML}$ | ToA estimate using the even ML estimator in (4.29) |
| $\hat{\tau}_{MC}$ | ToA estimate using the MC estimator in (2.24) |

| | |
|---|---|
| $\hat{\tau}_{\mathrm{ML}}$ | ToA estimate using the ML estimator in (1.2) |
| $\hat{\tau}_{\mathrm{OML}}$ | ToA estimate using the odd ML estimator in (4.29) |
| $\tau_{n_P}$ | ToA of the $n_P$-th multipath component in (1.7) |
| $\boldsymbol{\tau}$ | vector of ToAs in (5.19) |
| $\bar{\boldsymbol{\tau}}$ | vector taken from the last $B - M$ elements of $\boldsymbol{\tau}$ in (6.3) |
| $\hat{\boldsymbol{\tau}}$ | estimate of $\boldsymbol{\tau}$ in (6.7) |
| $\hat{\bar{\boldsymbol{\tau}}}$ | estimate of $\bar{\boldsymbol{\tau}}$ in (6.7) |
| $\theta$ | AoD in Sec. 8.4.1 |
| $\boldsymbol{\theta}$ | unknown parameter in (4.11) |
| $\boldsymbol{\theta}$ | vector defined in (8.25d) |
| $\boldsymbol{\theta}_0$ | true value of model parameter in (5.20) |
| $\boldsymbol{\theta}_{\check{\alpha}}$ | unknown parameter for complex-valued unstructured model in (4.25) |
| $\boldsymbol{\theta}_\gamma$ | unknown parameter in complex-valued path loss model in (4.28) |
| $\boldsymbol{\theta}_{\check{\gamma}}$ | unknown parameter for complex-valued path loss in (4.31) |
| $\hat{\boldsymbol{\tau}}_{\mathrm{ML}}$ | ML estimate of the ToA from all multipath components in (1.14) |
| $\boldsymbol{\Theta}$ | matrix defined in (8.26d) |
| $\boldsymbol{\Theta}[k, l]$ | matrix defined in (8.27d) |
| $\upsilon[k, l]$ | phase shift of the $k$-th component in the $l$-th cluster in (8.7) |
| $\boldsymbol{\upsilon}$ | vector defined in (8.25b) |
| $\boldsymbol{\Upsilon}$ | matrix defined in (1.26a) |
| $\boldsymbol{\Upsilon}$ | matrix defined in (8.26b) |
| $\boldsymbol{\Upsilon}[k, l]$ | matrix defined in (8.27b) |
| $\varepsilon_1(\tau_0, \gamma_0)$ | a quantity defined in (4.46a) |
| $\varepsilon_2(\tau_0)$ | a quantity defined in (4.46b) |
| $\varepsilon_{\mathrm{CRB}}(\tilde{\sigma})$ | total error in both axes by CRB in (7.38) |
| $\varepsilon_{\mathrm{ACRB}}$ | estimation error of the mobile position from both axes by ACRB in (7.67a) |
| $\varepsilon_{\mathrm{BCRB}}$ | estimation error of the mobile position from both axes by SBCRB in (7.67c) |
| $\varepsilon_{\mathrm{SBCRB}}$ | estimation error of the mobile position from both axes by SBCRB in (7.67b) |
| $\varpi$ | quantity defined in (7.45) |
| $\varphi_i(t)$ | orthonormal basis function in (1.31) |
| $\varphi(t, \acute{t})$ | eigenfunction, which is noise autocovariance function, in (2.14) |
| $\varphi_b(t, \acute{t})$ | eigenfunction at the $b$-th BS in (5.10) |
| $\boldsymbol{\Xi}(f)$ | Fourier transform of the channel matrix in (1.38) |
| $\boldsymbol{\zeta}$ | vector defined in (1.26c) |
| $\hat{\mathbf{q}}_{\mathrm{LLS}}$ | linearlized least squares estimate in (1.27) |
| $\xi_b$ | shadow fading at the $b$-th BS in (7.1) |
| $\tilde{\xi}$ | random shadow fading in (7.37) |
| $\zeta(\tau)$ | ML objective function in (2.31) |
| $\simeq$ | approximation by neglecting $o(\cdot)$ in (2.22) |
| $*$ | convolution in (8.1) |
| $\odot$ | Hadamard product in (7.7) |
| $\frac{\partial}{\partial t}$ | partial derivative with respect to $t$ |
| $\lVert \cdot \rVert_E$ | Euclidean norm |

| | |
|---|---|
| $(\cdot)^*$ | complex conjugate of $\cdot$ |
| $\lvert\cdot\rvert$ | absolute value of scalar $\cdot$, or determinant of matrix $\cdot$ |
| $\lfloor\cdot\rfloor$ | least integer number of $\cdot$ |
| $(\cdot)^{-1}$ | inverse of matrix $\cdot$ |
| $\mathbf{B} \succeq \mathbf{C}$ | difference matrix $\mathbf{A} = \mathbf{B} - \mathbf{C}$ is positive semidefinite |
| $\arg\max_{\tau} f(\tau)$ | argument $\tau$, which maximizes the objective function $f(\tau)$, in (2.24) |
| $\arg\min_{\tau} f(\tau)$ | argument $\tau$, which minimizes the objective function $f(\tau)$, in (2.33) |
| $\arg\operatorname{zero}_{\tau} f(\tau)$ | argument $\tau$, which makes the objective function $f(\tau)$ zero, in (3.31) |
| $\mathrm{E}_{n(\cdot)}\{\cdot\}$ | expectation with respect to the realization of $n(\cdot)$ in (2.28) |
| $\operatorname{erf}(\cdot)$ | error function in (3.23) |
| $f(x)\vert_{x=x_0}$ | function $f(x)$ evaluated at $x = x_0$ |
| $\mathrm{I}_0(\cdot)$ | zeroth order modified Bessel function of the first kind in (4.48a) |
| $\mathrm{I}_k(\cdot)$ | k-th order modified Bessel function of the first kind in (4.48b) |
| $\Im(\cdot)$ | imaginary part of $\cdot$ |
| $\ln(\cdot)$ | natural logarithm function in (3.9) |
| $\log_{10}(\cdot)$ | logarithm of base 10 |
| $\max_{x} f(x)$ | maximum value of the function $f(x)$ over the set of $x$ in (8.2) |
| $[\mathbf{M}]_{[2\times 2]}$ | the first $2 \times 2$ block of $\mathbf{M}$ |
| $\Re(\cdot)$ | real part of $\cdot$ |
| $\operatorname{sinc}(\cdot)$ | unnormalized sine cardinal function in (2.40) |
| $\operatorname{tr}(\cdot)$ | trace of matrix $\cdot$ |
| $\operatorname{vec}(\cdot)$ | column-stacking vectorization in (8.25) |